The influence of the trapping potential on the attachment of a second electron to stored metal cluster and fullerene anions

A. Herlert [a,*], R. Jertz [b], J. Alonso Otamendi [a,c], A.J. González Martínez [a,c], L. Schweikhard [d]

[a] *Institut für Physik, Johannes Gutenberg-Universität, D-55099 Mainz, Germany*
[b] *Bruker-Daltonik GmbH, Fahrenheitstraße 4, D-28359 Bremen, Germany*
[c] *Facultad de Física, Universidad de Valencia, Dr. Moliner 50, 46100 Burjassot, Spain*
[d] *Institut für Physik, Ernst-Moritz-Arndt-Universität, D-17487 Greifswald, Germany*

Abstract

Singly charged anionic clusters are exposed to a bath of simultaneously stored electrons in ion cyclotron resonance (Penning) traps and thus, dianions are produced. The dianion yield is found to be a function of the potential well depth. As an example, the attachment of electrons to size-selected gold cluster anions Au_{25}^{1-} from a laser vaporization source has been studied in detail by time-of-flight mass analysis after ejection of all ions from the trap. Furthermore, the investigation is extended to fullerene anions C_{70}^{1-} that are produced by laser desorption from a fullerene target in the external source of a Fourier-transform ion cyclotron resonance (FT-ICR) mass spectrometer. As in the case of metal cluster dianions, the possibility to add another surplus electron depends on the potential well depth, presumably due to the repulsive Coulomb barrier for electron attachment. The threshold of the potential well depth has been determined to be about 2.5 V for the production of Au_{25}^{2-} in a hyperbolical Penning trap and 5.8 V for the formation of C_{70}^{2-} in a cylindrical FT-ICR trap. (Int J Mass Spectrom 218 (2002) 217–225) © 2002 Elsevier Science B.V. All rights reserved.

1. Introduction

Doubly charged systems have attracted much interest in the last years [1,2]. Gas-phase dianions were observed by use of different experimental techniques. Ion beam sputtering sources produced dianions of small carbon clusters [3], silicon–carbon clusters [4], beryllium–carbon clusters [5,6], and alkaline-earth metal tetrahalides [7]. Doubly charged fullerene anions were observed after laser desorption from a target [8,9], and by use of electrospray ionization sources fullerenes [10,11] as well as metal tetrahalides [12,13] and alkali halide clusters [14] were produced.

In addition, the subsequent charging of neutral fullerenes [15] and highly fluorinated fullerenes [16] with two electrons has been reported. In the first case, the charging was performed in the ion source of a hybrid magnetic-sector quadrupole mass spectrometer, where 70-eV electrons were moderated by nitrogen gas. For the fluorinated fullerenes ion trapping in an ICR cell has been used and "low-energy electrons from an electron beam" were applied. In this particular case, the main dianion formation pathway observed was dissociative attachment.

* Corresponding author. E-mail: alexander.herlert@uni-mainz.de

With a similar approach gold cluster dianions have been observed in a Penning trap mass spectrometer [17,18] after application of a bath of simultaneously stored electrons. After these first observations of doubly charged metal cluster anions, multiply charged anionic metal clusters have also been reported for laser desorption of metal targets under high vacuum conditions [19].

The details of the attachment processes in the electron bath are still under investigation. In the present work, the influence of the trapping potential is studied in more detail. To this end, gold cluster anions Au_{25}^{1-} are subjected to an electron bath and the yield of produced dianions is measured as a function of the applied trapping potential well depth.

In addition, the method of charging pre-selected species stored in a trap has been transferred to a commercial Fourier-transform ion cyclotron resonance (FT-ICR) mass spectrometer and applied to fullerene anions C_{70}^{1-}. Already a decade ago doubly charged fullerene anions had been observed after laser desorption from a target close to the FT-ICR trap volume [8,9]. However, these early measurements were not concerned about the production mechanisms of the new species and the addition of another electron to singly charged fullerene anions has not yet been performed under controlled conditions.

2. Gold clusters

2.1. Experimental setup and procedure

The gold cluster measurements have been performed in the "Cluster Trap". This experimental setup has been reported in detail elsewhere [20,21]. In brief, singly charged gold cluster anions are produced in an external Smalley-type laser-vaporization source [22,23]. Material is evaporated from a gold wire and partially ionized by use of a frequency doubled pulsed Nd:YAG laser ($\lambda = 532\,nm$, 5–10 mJ). The plasma is cooled by a helium gas pulse and the helium/cluster mixture is expanded adiabatically through a nozzle into the vacuum. Neutral and singly charged clusters,

both cations and anions are produced in this process, but no doubly charged ions. (Doubly charged atomic cations of titanium, Ti^{2+}, are the only exception observed so far.) The negatively charged gold clusters are accelerated and guided by ion-optical elements toward the hyperbolically shaped Penning trap [24] (with trap dimensions $2r_0 = 40\,mm$ and $2z_0 = \sqrt{2}r_0$ for the open diameter of the ring electrode and the distance between the endcaps, respectively, magnetic field $B = 5\,T$, and trapping voltage $U_0 = 4$–$22\,V$ between endcaps and ring electrode). The cluster anions are captured in flight [25], size selected by radial ejection of all unwanted ions and stored for further experimental investigations [26,27].

In the specific case of electron attachment, the beam of an external electron gun is guided through the trap, while argon gas is pulsed into the trap region (beam duration 1 s, kinetic energy of electrons about 40 eV). Argon atoms are ionized and thus, secondary low-energy electrons are produced. Due to the trapping conditions the positively charged argon atoms leave the trap whereas the secondary electrons are stored together with the previously captured gold cluster anions. Eventually, electrons attach to the cluster anions, i.e., dianions are produced [17,18,28,29]. For mass analysis, the stored particles are ejected out of the trap into a drift region for time-of-flight (TOF) mass spectrometry. Fig. 1 shows typical spectra after electron attachment to size-selected gold clusters
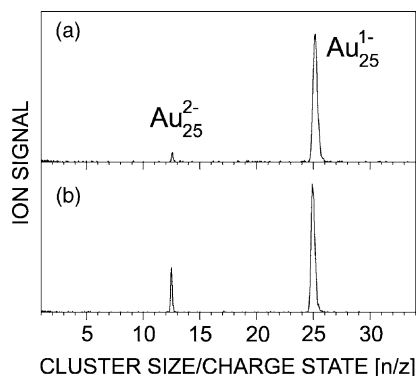

Fig. 1. TOF mass spectra after electron attachment to size-selected gold clusters Au_{25}^{1-} at a trapping potential depth of (a) $U_T = 4\,V$ and (b) $U_T = 7\,V$.

Au_{25}^{1-}. The signal of the dianion Au_{25}^{2-} appears at half of the mass-over-charge ratio of the precursor in the mass spectrum, i.e., at $n/z = 12.5$.

2.2. Dianion signal intensity as a function of the potential well depth

The relative dianion yield after electron attachment has been measured as a function of the trapping potential depth U_T (see below), while all other experimental parameters have been kept fixed. As an example, two mass spectra measured at (a) $U_T = 4$ V and (b) $U_T = 7$ V are shown in Fig. 1. Obviously, the dianion yield strongly depends on the trapping voltage. For an ideal Penning trap with hyperbolically shaped electrodes the trapping potential is given by [24]

$$U(r, z) = U_0 \frac{z^2 - r^2/2}{2d_0^2}, \qquad (1)$$

where U_0 is the potential difference between the endcaps and the ring electrode (which is negative in the case of anions) and d_0 is the trap dimension defined as $d_0^2 := (z_0^2 + r_0^2/2)/2$. By the use of Eq. (1), the potential well depth U_T along the z-axis is $U_T = U_0 z_0^2/(2d_0^2) = U_0/2$ for the present case of an asymptotically symmetric trap ($r_0^2 = 2z_0^2$, [24,30]).

In Fig. 2, the relative abundance of dianions Au_{25}^{2-}, that are produced by electron attachment to singly charged gold clusters Au_{25}^{1-}, is plotted as a function
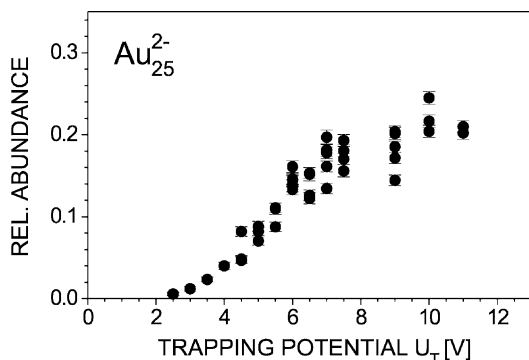

Fig. 2. Relative abundance of dianions Au_{25}^{2-} as a function of the well depth U_T of the trapping potential.

of the trapping potential well depth U_T, which has been varied between 2 and 11 V. The dianion signal starts to appear at $U_T \approx 2.5$ V and increases to a relative yield of about 20% for $U_T \approx 8$ V, where it levels off. The error bars give the statistical uncertainty of each measurement. Fig. 2 also shows the day-to-day variance. These larger fluctuations are due to the limited reproducibility of the experimental parameters, in particular for the production of the electron bath.

3. Fullerenes

3.1. Experimental setup and procedure

The method of charging singly charged ions by use of an electron bath in an ion trap has been extended to fullerenes and a commercial Fourier-transform ion cyclotron resonance mass spectrometer (FT-ICR MS) APEX II, manufactured by Bruker Daltonics (Billerica, MA, USA) as described in the following. A cylindrical "infinity" cell [31] (length 60 mm, diameter 60 mm) is positioned inside a 4.7-T actively shielded superconducting magnet. A newly designed ion source for matrix-assisted laser desorption ionization (MALDI) which is described in detail elsewhere [32] has been attached to the external source chamber of the FT-ICR MS instrument. This ion source is connected to the ICR cell via a cylindrical ion optical system which is differentially pumped by a set of three turbo molecular pumps. A base pressure of about 10^{-10} mbar can be achieved in the cell region.

The C_{70} fullerene target is prepared by dissolving a C_{70} powder (FLUKA 18832, Buckminsterfullerene C_{70}) in toluene. Some microliters of this solution is put onto the target surface and dried by a heating gun. This method provides a thick layer of C_{70} fullerenes which results in strong fullerene ion signals.

Fullerene anions C_{70}^{1-} are created by firing a nitrogen laser ($\lambda = 337$ nm, 200 μJ per pulse) onto the target. Ions from one or several laser shots can be captured and cooled by collisions with argon gas (up to pressures of the order of 10^{-2} mbar in the vicinity of the laser target) in a hexapole ion guide. The ions

are then accelerated to 3 keV and transferred to the ICR cell. The potential of the front trapping plate of the ICR cell is decreased and the ions enter the trap via a 5 mm diameter hole in the center of the plate. The opening time depends on the mass of the trapped ion species which discriminates the lower and upper limit of a certain mass range. After raising the trapping plate potential the ions are captured.

By use of a high-amplitude dipolar-excitation isolation sweep all unwanted ion species captured together with C_{70}^{1-} are ejected out of the ICR cell. The electron bath is created in full analogy to the gold-cluster experiments: Argon gas is pulsed into the trap region by a pulsed valve that is directly attached to the UHV system. By use of electrons from a heated rhenium filament ($E = 70$ eV, $\Delta t = 100$ ms) which is placed on the magnetic field axis opposite to the entrance trapping plate and about 15 cm from the trap center, argon atoms are ionized and secondary electrons are produced. While the positively charged ions are lost, the electrons stay trapped in the cell together with the C_{70}^{1-} anions which may capture an electron to form dianions.

The reaction products are detected by use of the FT-ICR technique (see [33] and references therein). The trapped ions are excited by a dipolar rf field which leads to a coherent motion of the ion cloud at a larger cyclotron orbit. This ion motion is detected via the image currents induced into the ring electrodes of the cell. This signal is amplified and digitized by use of a transient recorder and transferred to a Silicon Graphics O2 computer, where it is Fourier transformed to obtain a frequency spectrum. The complete experiment control which includes timing, voltage setting, and data acquisition is performed by use of the Bruker Daltonics Xmass® software.

3.2. Identification of the dianion signal

In Fig. 3(a) a frequency spectrum of isolated C_{70}^{1-} is shown. In addition to the fullerene anion signal, two other signals appear in the spectrum. They are observed at the third (Fig. 3(b)) and second harmonic of the reduced cyclotron frequency of C_{70}^{1-} (Fig. 3(c)).
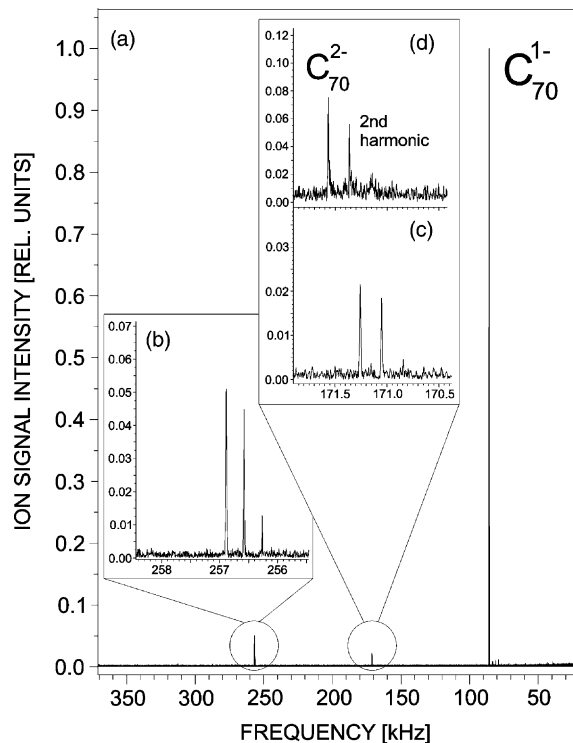

Fig. 3. FT-ICR frequency spectrum of isolated fullerenes C_{70}^{1-} (a) at a trapping voltage of $U_0 = 9.9$ V. The third harmonic (b) and the second harmonic (c) of the anion signal are magnified (and the isotopomeric structure of C_{70}^{1-} is resolved). After application of an electron bath to the stored fullerenes (d) C_{70}^{2-} appears as an additional signal in the frequency spectrum.

Note, that isotopomers of C_{70}^{1-} are observed. However, only the signal of $^{12}C_{70}$ is analyzed in the following. The high resolving power of the FT-ICR detection technique allows to distinguish between the actual dianion signal C_{70}^{2-} at its reduced cyclotron frequency and the second harmonic of the C_{70}^{1-} oscillation frequency (see Fig. 3(d)). For the identification of the dianion signal, the reduced cyclotron frequency of the dianion C_{70}^{2-} as well as the second harmonic of the anion oscillation is measured as a function of the applied trapping voltage U_0. As shown earlier [9] the behavior of the signal frequencies as a function of the trapping potential allows the identification of the signals. In the following, this method is reviewed for the present case.

The cyclotron frequency $\omega_c = qB/m$ of a particle of mass m and charge q in a magnetic field B is shifted due to the quadrupolar electrostatic trapping potential. Thus, the ions revolve at a reduced cyclotron frequency [24,34]:

$$\omega_+ = \frac{\omega_c}{2}\left(1 + \sqrt{1 - 2\frac{\omega_z^2}{\omega_c^2}}\right), \tag{2}$$

where $\omega_z = \sqrt{qU_0/md_0^2}$ is the axial oscillation frequency. Since ω_z is small compared to ω_c, Eq. (2) can be Taylor-expanded and approximated by

$$\omega_+ \approx \omega_c - \frac{1}{2}\frac{\omega_z^2}{\omega_c} = \omega_c - \Delta\omega, \tag{2'}$$

with the shift $\Delta\omega = U_0/2Bd_0^2$. Thus, in this case the reduced cyclotron frequency ω_+ depends linearly on the applied trapping voltage U_0. For the present experimental parameters, the shift is given by $\Delta\nu = \Delta\omega/2\pi = U_0 \times 27\,\text{Hz/V}$. With Eq. (2'), the frequency of the nth harmonic of the fullerene anion signal is

$$n\omega_+ \approx n\omega_c - n\,\Delta\omega, \tag{3}$$

and thus, the frequency shift as a function of trapping voltage U_0 of the nth harmonic is n times the shift of any "real" ion signal frequency, as, e.g., that of the mono-anion. In Fig. 4, the measured signal frequencies of (a) C_{70}^{1-} (circles), (b) the second and (c) the third harmonic (triangles) are plotted as a function of the trapping voltage U_0. Open symbols denote measurements performed without an electron bath. The solid lines are linear fits to the data with the slopes 26.5(7), 53.0(14) and 79.7(20) Hz/V for the anion signal, the second and the third harmonic, respectively, in very good agreement with the predicted value.

After the application of an electron bath, the signal frequency of C_{70}^{1-} (see Fig. 4(a), full symbols) is shifted by a constant value of about 50 Hz to larger frequencies compared to the measurements without electron bath (open symbols). A linear fit (Fig. 4(a), dashed line) yields a slope of 24.0(14) Hz/V, which is slightly smaller than the predicted value, but still in good agreement. The signal frequency of the second
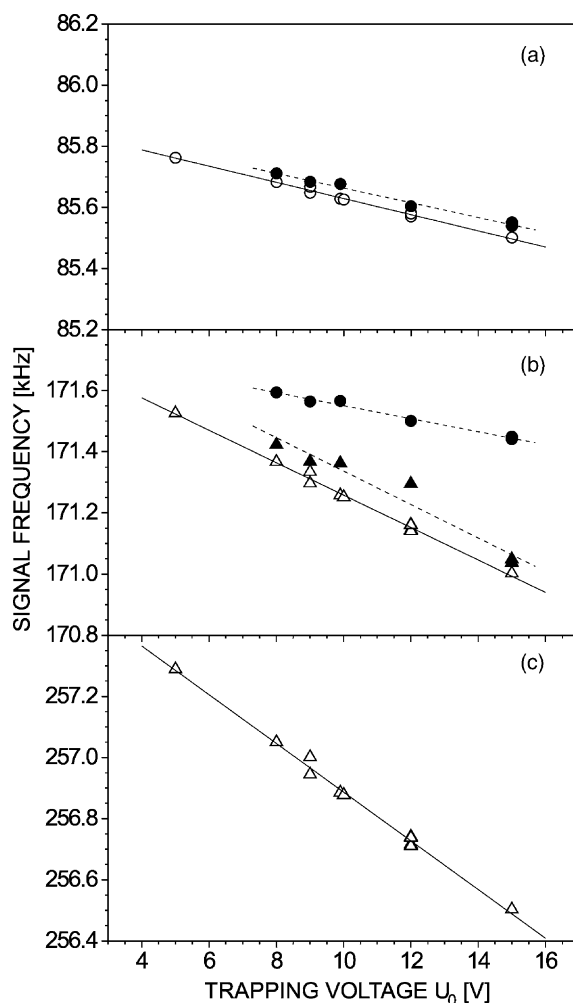

Fig. 4. Signal frequency of (a) C_{70}^{1-}, (b) the second harmonic of C_{70}^{1-} (triangles) and the dianion C_{70}^{2-} (circles), and (c) the third harmonic of C_{70}^{1-} as a function of the trapping voltage U_0. Open symbols are measurements without and full symbols measurements after application of an electron bath. (the error bars, i.e., the FWHM of the signals, are smaller than the symbol size).

harmonic is also shifted to larger values (Fig. 4(b), full triangles), but a linear fit results in a slope of 55(6) Hz/V as expected from Eq. (3). The space charge due to the stored electrons is expected to shift the reduced cyclotron frequency to smaller frequencies [35] rather than to the observed larger frequencies. The origin of this small constant shift is as yet unknown, but for the signal identification it is not significant.

The additional signal (Fig. 4(b), full circles), that appears at about two times the cyclotron frequency of C_{70}^{1-} in the frequency spectrum after application of an electron bath, shows a much smaller frequency shift $\Delta\omega$ than the second harmonic (Fig. 4(b), full triangles) and can therefore, easily be distinguished. A linear fit (dashed line) yields a value of 21.3(13) Hz/V, which is in good agreement with the frequency shift Δn of the C_{70}^{1-} signal. Thus, the additional signal can be unambiguously identified with the signal of the dianion C_{70}^{2-}.

3.3. Dianion signal intensity as a function of the potential well depth

As in the case of the gold clusters in the Penning trap, the measurements on fullerene dianions have been performed for different trapping voltages U_0, i.e., for different potential well depths U_T. The trapping potential of a closed cylindrical cell has been calculated in, e.g. [36]. In the center of the trap it can be approximated by

$$U(r, z) = \gamma U_0 + \alpha U_0 \frac{z^2 - r^2/2}{r_0^2} + O(4), \qquad (4)$$

where for a trap with unit aspect ratio (in the present case $r_0 = z_0 = 30$ mm) the geometrical factors are $\gamma = 0.2787$ and $\alpha = 2.8404$ [37]. This yields a potential well depth in the axial direction of $U_T = (1 - \gamma)U_0 \approx 0.72 U_0$.

Since the dianions have twice the charge, the intensity of the FT-ICR signal intensity I is two times larger than that of the mono-anion signal. Thus, the relative dianion abundance is given by

$$\frac{I(C_{70}^{2-})}{I(C_{70}^{2-}) + 2I(C_{70}^{-})}. \qquad (5)$$

Fig. 5 shows this corrected relative dianion abundance as a function of the potential well depth U_T. The dianions are observed for a potential well depth U_T in excess of about 5.8 V. Note, that while there is a gradual increase of the gold-dianion signal (Fig. 2) the fullerene dianion signal appears rather abrupt. Below
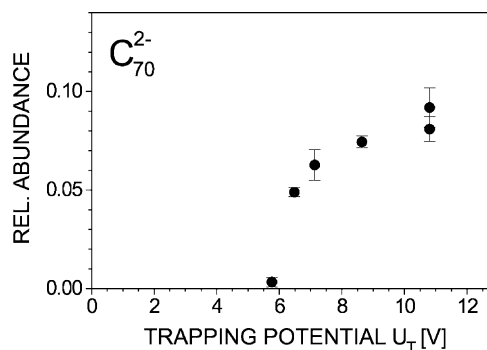
Fig. 5. Relative abundance of fullerene dianions C_{70}^{2-} as a function of the well depth U_T of the trapping potential.

$U_T = 5.8$ V no dianion signal has been observed. Thus, the threshold is at about 5.8 V or just below.

4. Discussion

In both cases, gold clusters Au_{25}^{1-} in a Penning trap and fullerenes C_{70}^{1-} in an FT-ICR cell, electrons have been attached to the anions and thus, dianionic systems have been formed. In order to achieve attachment the electrons have to overcome the repulsive Coulomb barrier of the singly charged cluster and fullerene anions, respectively. In Fig. 6, the Coulomb
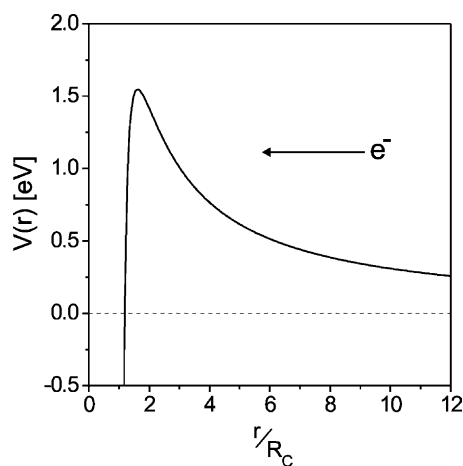
Fig. 6. Coulomb potential of a singly charged gold cluster Au_{25}^{1-} as seen by an approaching electron. Approximation for a conducting sphere including the polarizability (see Eq. (6)).

potential of a gold cluster $Au_{25}{}^{1-}$ with respect to a singly charged particle such as an electron is plotted as a function of the radial distance. The cluster anion is approximated by a sphere with a radius $R_C = R_0 n^{1/3}$, where $R_0 = 1.59\,\text{Å}$ is the Wigner–Seitz radius of a gold atom and n is the number of atoms in the cluster, i.e., $R_C = 4.65\,\text{Å}$ for the present case of $n = 25$. The Coulomb potential is given by

$$V(r) = \frac{e^2}{4\pi\varepsilon_0}\left(\frac{1}{r} + \frac{R_C}{2r^2} - \frac{R_C}{2(r^2 - R_C^2)}\right). \qquad (6)$$

This approximation assumes a perfect conducting sphere and includes the effect of the image charge, i.e., the polarizability of the cluster [18,38]. The Coulomb potential reaches a maximum $V_B = e^2/(8\pi\varepsilon_0 R_C) = 1.55\,\text{eV}$ at $R_B = 7.54\,\text{Å}$. An electron has to overcome the Coulomb barrier in order to attach to the cluster anion (where the surplus energy is dissipated and thus the electron is left trapped inside the cluster). Therefore, neglecting any tunneling, the minimum kinetic energy of the electrons required for attachment is $1.55\,\text{eV}$.

The fullerene anions $C_{70}{}^{1-}$ are not spherical but deformed like a "rugby ball". However, the deformation is small with principal axes of 7.96 and $7.12\,\text{Å}$ [39]. Thus, in the following the Coulomb barrier is approximated by a spherical shape with a radius of $R_C = 3.77\,\text{Å}$. From Eq. (6) this yields a Coulomb barrier of $V_B = 1.91\,\text{eV}$.

To compare the calculated potential barriers with the observed threshold values for the attachment of another surplus electron, the kinetic energy distribution of the electron bath has to be further investigated. During the ionization of argon atoms by the electron beam, secondary electrons are produced with an unknown distribution of the kinetic energy along the beam line of the primary electrons. For a given potential well depth, electrons with a kinetic energy $E > eU_T$ in the trapping mode may axially leave the trap. This gives an upper limit of the axial kinetic energy distribution of the electrons. In addition, the cyclotron motion of the electrons in the Penning trap is damped by radiative cooling. For an ideal Pen-

ning trap, the cyclotron energy decays exponentially [24,40] with the cyclotron damping constant

$$\gamma_c = \frac{1}{4\pi\varepsilon_0}\frac{4e^2\omega_c^2}{3mc^3}. \qquad (7)$$

For the given experimental parameters $\gamma_c = 9.68\,\text{s}^{-1}$ or $\gamma_c^{-1} \approx 0.1\,\text{s}$. Thus, radiative cooling is an important cooling mechanism. Similar to the cyclotron motion the damping constant of the axial motion is given by [24]

$$\gamma_z = \frac{1}{4\pi\varepsilon_0}\frac{2e^2\omega_z^2}{3mc^3}, \qquad (8)$$

which leads to a value of $\gamma_z^{-1} \approx 1.5 \times 10^7\,\text{s}$ and therefore, radiative cooling can be neglected for the axial as well as the magnetron motion (since its frequency is several orders of magnitude smaller than ω_z). However, the Coulomb interaction between the electrons in the trap may lead to a transfer of the axial energy of the electrons to the radial motion that is then cooled due to radiative damping of the cyclotron motion.

Due to the loss of electrons in the axial direction and the fast damping of the radial motion of the electrons, the typical kinetic energy of the secondary electrons drops rather fast to only a fraction of the maximum value of the potential well depth. Thus, the threshold well depth for the efficient production of dianions has to be considerably larger than the Coulomb barrier in agreement with the present observation.

5. Conclusion and outlook

For the first time details of the attachment of an additional electron to stored singly charged cluster ions have been studied. To this end, gold cluster anions $Au_{25}{}^{1-}$ and fullerene anions $C_{70}{}^{1-}$ were trapped in a bath of electrons. The yield of dianions produced from mono-anions was observed to depend on the well depth of the trapping potential. The threshold of dianion production has been determined to be $U_T \approx 2.5\,\text{V}$ for $Au_{25}{}^{2-}$ in a hyperbolical Penning trap and $U_T \approx 5.8\,\text{V}$ for $C_{70}{}^{2-}$ in a cylindrical FT-ICR trap. These observations can be related to the repulsive

Coulomb barrier of the singly charged species, that has to be overcome by the second surplus electron in order to attach. The potential well depth has to be larger than the Coulomb barrier, such that a sufficient number of electrons has the kinetic energy necessary for the attachment process. In view of the relative small difference of the Coulomb barrier height of the gold clusters and the fullerenes, it remains an open question why these species differ a lot with respect to their respective threshold potential well depth for dianion observation. There may be some influence from the experimental techniques that have been adopted for the two different experiments. We plan to perform cross reference measurements in the future in order to explore this possibility.

However, it has been shown by the present study that the application of an electron bath allows to attach further electrons to anionic systems of interest with commercially available FT-ICR mass spectrometers. This happens in the same way as introduced in the custom-designed "cluster trap"—provided appropriate trapping potentials are applied. In both cases, the mass selection in the trap prior to the attachment process allows the production of doubly charged systems without the overlap of anions with the same mass over charge ratio. The properties of metal cluster dianions are currently investigated by use of laser excitation [41,42] as well as collisional activation [43] where some special care has to be taken with respect to the ions' radial motion [44]. It is also planned to continue to study the stability of the doubly charged fullerene anions C_{70}^{2-} with respect to electron autodetachment as shown in the case of C_{84}^{2-} [15]. The possibility of varying the storage time in an ion-trap experiment over many orders of magnitude allows the investigation of metastable dianions as reported in the case of $PtCl_4^{2-}$ [45]. Recent measurements on C_{70}^{2-} showed a half-life of about 80 s [11]. It may be worth noting that the fullerene dianion C_{60}^{2-} which had been reported earlier [8,9] has not yet been observed by the present method despite several trials. The stability of C_{60}^{2-} is of special interest, since the electron affinity of the anion C_{60}^{1-} is reported to be close to zero [8,10,46].

References

[1] M.K. Scheller, R.N. Compton, L.S. Cederbaum, Science 270 (1995) 1160.
[2] A. Dreuw, L.S. Cederbaum, Chem. Rev. 102 (2002) 181.
[3] S.N. Schauer, P. Williams, R.N. Compton, Phys. Rev. Lett. 65 (1990) 625.
[4] H. Gnaser, Phys. Rev. A 60 (1999) R2645.
[5] J. Klein, R. Middleton, Nucl. Instrum. Meth. B 159 (1999) 8.
[6] D. Berkovits, O. Heber, J. Klein, D. Mitnik, M. Paul, Nucl. Instrum. Meth. B 172 (2000) 350.
[7] R. Middleton, J. Klein, Phys. Rev. A 60 (1999) 3515.
[8] R.L. Hettich, R.N. Compton, R.H. Ritchie, Phys. Rev. Lett. 67 (1991) 1242.
[9] P.A. Limbach, L. Schweikhard, K.A. Cowen, M.T. McDermott, A.G. Marshall, J.V. Coe, J. Am. Chem. Soc. 113 (1991) 6795.
[10] G. Khairallah, J.B. Peel, Chem. Phys. Lett. 296 (1998) 545.
[11] O. Hampe, M. Neumaier, M.N. Blom, M.M. Kappes, Chem. Phys. Lett. 354 (2002) 303.
[12] X.-B. Wang, L.-S. Wang, Phys. Rev. Lett. 83 (1999) 3402.
[13] P. Weis, O. Hampe, S. Gilb, M.M. Kappes, Chem. Phys. Lett. 321 (2000) 426.
[14] J. Friedrich, P. Weis, J. Kaller, R.L. Whetten, M.M. Kappes, Eur. Phys. J. D 9 (1999) 269.
[15] R.N. Compton, A.A. Tuinman, C.E. Klots, M.R. Pederson, D.C. Patton, Phys. Rev. Lett. 78 (1997) 4367.
[16] C. Jin, R.L. Hettich, R.N. Compton, A. Tuinman, A. Derecskei-Kovacs, D.S. Marynick, B.I. Dunlap, Phys. Rev. Lett. 73 (1994) 2821.
[17] A. Herlert, S. Krückeberg, L. Schweikhard, M. Vogel, C. Walther, Phys. Scripta T80 (1999) 200.
[18] L. Schweikhard, A. Herlert, S. Krückeberg, M. Vogel, C. Walther, Philos. Mag. B 79 (1999) 1343.
[19] C. Stoermer, J. Friedrich, M.M. Kappes, Int. J. Mass Spectrom. 206 (2001) 63.
[20] St. Becker, K. Dasgupta, G. Dietrich, H.-J. Kluge, S. Kuznetsov, M. Lindinger, K. Lützenkirchen, L. Schweikhard, J. Ziegler, Rev. Sci. Instrum. 66 (1995) 4902.
[21] L. Schweikhard, St. Becker, K. Dasgupta, G. Dietrich, H.-J. Kluge, D. Kreisle, S. Krückeberg, S. Kuznetsov, M. Lindinger, K. Lützenkirchen, B. Obst, C. Walther, H. Weidele, J. Ziegler, Phys. Scripta T59 (1995) 236.
[22] T.G. Dietz, M.A. Duncan, D.E. Powers, R.E. Smalley, J. Chem. Phys. 74 (1981) 6511.
[23] H. Weidele, U. Frenzel, T. Leisner, D. Kreisle, Z. Phys. D 20 (1991) 411.

[24] L.S. Brown, G. Gabrielse, Rev. Mod. Phys. 58 (1986) 233.

[25] H. Schnatz, G. Bollen, P. Dabkievicz, P. Egelhof, F. Kern, H. Kalinowsky, L. Schweikhard, H. Stolzenberg, H.-J. Kluge, The ISOLDE Collaboration, Nucl. Instrum. Meth. A 251 (1986) 17.

[26] L. Schweikhard, S. Krückeberg, K. Lützenkirchen, C. Walther, Eur. Phys. J. D 9 (1999) 15.

[27] L. Schweikhard, A. Herlert, M. Vogel, Metal clusters as investigated in a Penning trap, in: E.E.B. Campbell, M. Larsson (Eds.), The Physics and Chemistry of Clusters (Proceedings of the Nobel Symposium 117), Visby, 27 June–2 July 2000, World Scientific, Singapore, 2001, pp. 267–277.

[28] A. Herlert, L. Schweikhard, M. Vogel, Eur. Phys. J. D 16 (2001) 65.

[29] C. Yannouleas, U. Landman, A. Herlert, L. Schweikhard, Phys. Rev. Lett. 86 (2001) 2996.

[30] R.D. Knight, Int. J. Mass Spectrom. Ion Process. 51 (1983) 127.

[31] P. Caravatti, M. Allemann, Org. Mass Spectrom. 26 (1991) 514.

[32] G. Baykut, R. Jertz, M. Witt, Rapid Commun. Mass Spectrom. 14 (2000) 1238.

[33] A.G. Marshall, C.L. Hendrickson, G.S. Jackson, Mass Spectrom. Rev. 17 (1998) 1.

[34] L. Schweikhard, J. Ziegler, H. Bopp, K. Lützenkirchen, Int. J. Mass. Spectrom. Ion Process. 141 (1995) 77.

[35] J.B. Jeffries, S.E. Barlow, G.H. Dunn, Int. J. Mass Spectrom. Ion Process. 54 (1983) 169.

[36] G. Gabrielse, F.C. MacKintosh, Int. J. Mass Spectrom. Ion Process. 57 (1984) 1.

[37] S. Guan, A.G. Marshall, Int. J. Mass Spectrom. Ion Process. 146/147 (1995) 261.

[38] J.D. Jackson, Classical Electrodynamics, 2nd Edition, Wiley, New York, 1975.

[39] M.S. Dresselhaus, G. Dresselhaus, P.C. Eklund, Science of Fullerenes and Carbon Nanotubes, Academic Press, San Diego, 1996.

[40] G.-Z. Li, S. Guan, A.G. Marshall, Am. Soc. Mass Spectrom. 8 (1997) 793.

[41] A. Herlert, K. Hansen, L. Schweikhard, M. Vogel, Hyperfine Interact. 127 (2000) 529.

[42] L. Schweikhard, G. Marx, K. Hansen, A. Herlert, M.D. Herráiz Lablanca, M. Vogel, Hyperfine Interact., in press.

[43] H. Weidele, M. Vogel, A. Herlert, S. Krückeberg, P. Lievens, R.E. Silverans, C. Walther, L. Schweikhard, Eur. Phys. J. D 9 (1999) 173.

[44] A. Herlert, L. Schweikhard, M. Vogel, Charge-changing reactions and their influence on the ion motion in a Penning trap, in: F. Anderegg, L. Schweikhard, C.F. Driscoll (Eds.), Non-Neutral Plasma physics IV (Proceedings of the Workshop on Non-Neutral Plasmas), San Diego, 30 July–2 August 2001, AIP Conference Proceedings 606, 2002, p. 652.

[45] M.N. Blom, O. Hampe, S. Gilb, P. Weis, M.M. Kappes, J. Chem. Phys. 115 (2001) 3690.

[46] C. Yannouleas, U. Landman, Chem. Phys. Lett. 217 (1994) 175.